Reactivity of Coordinatively Unsaturated Trivalent Chromium Complexes with Sulfur: Preparation of Novel Sulfide-Bridged Dinuclear Cr^{IV} Derivatives

Damien Reardon, Istvan Kovacs, Kamalesh B. P. Ruppa, Khalil Feghali, Sandro Gambarotta,* and Jeffrey Petersen*

Abstract: The homoleptic Cr^{III} amide complexes $[(RR'N)_3Cr]$ [R = R′ = cyclohexyl (**1a**); R = adamantyl, R′ = 3,5-Me_2Ph (**1b**)] were prepared and characterized. Reactions with elemental sulfur produced the corresponding dinuclear complexes $[\{(RR'N)_2Cr\}_2(\mu\text{-}S)_2]$ (**2**) through loss of one amide group. These two new dinuclear Cr^{IV} species are paramagnetic with magnetic moments lower than expected for the d^2 electronic configuration of Cr^{IV}. Magnetic measurements and ab initio calculations were carried out to elucidate the nature of magnetic interactions in these dinuclear systems. The molecular structures of **1a** and **2a** were elucidated by X-ray crystal structures.

Keywords
ab initio calculations · chromium · coordinative unsaturation · magnetic properties · sulfur

Introduction

In striking contrast to the extensive organometallic and coordination chemistry reported for trivalent chromium,[1] information about complexes containing chromium in the oxidation states +4 and +5 is scarce and limited to a few diverse complexes.[2, 3] For a long time this lacuna in the chemical literature[4] was ascribed to an intrinsic instability of these oxidation states. However, a recent revival of interest in this field has shown that the oxidation state +4 is more accessible and stable than previously thought.[3e, 5] This is a rather interesting development because these species are normally expected to easily disproportionate or reductively eliminate towards the most stable trivalent state. This implies that the redox couples Cr^{III}/Cr^{IV} and Cr^{III}/Cr^{V} may be particularly useful for catalytic purposes[6] related to oxidation[6b] and desulfurization reactions. Another stimulus to study this chemistry is provided by the rather important role played by these species in the biochemistry of chromium[7] in relation to the mechanism of toxicity and carcinogenic activity[8] of this metal, a topic of continuous interest.

Anionic organic amides have proven to be versatile supporting ligands for the stabilization of unstable oxidation states and the trapping of rare functionalities.[9] In particular, sterically demanding amides have allowed a number of interesting transformations. A notable example is a mononuclear derivative of Mo^{III} that is able to convert dinitrogen into nitride.[10] Although this type of reaction is apparently not observed with the chromium analogue, still coordinatively unsaturated Cr^{III} derivatives are able to denitrogenate nitrogen oxides.[11] This remarkable behavior suggested to us that triangular Cr^{III} amides could potentially be versatile reagents. However, little is known about the chemical reactivity of these species.[11b, c] Therefore, following our interest in the chemistry of Cr^{IV} derivatives,[12] we have now prepared several sterically encumbered chromium(III) tris(amide) complexes and have begun to evaluate their reactivity with oxidizing agents to form Cr^{IV} or Cr^{V} derivatives. The goal is twofold. First, we are interested in studying the possibility of increasing the reactivity of relatively inert trivalent chromium species through coordinative unsaturation. Second, we are interested in probing the stability of Cr^{IV} species. Our subsequent investigations of the reaction of sulfur with chromium(III) tris(amide) complexes have resulted in the isolation of d^2 Cr^{IV} sulfide-bridged dinuclear complexes. The results of our synthetic work, structural characterization, and magnetic susceptibility measurements are reported herein.

Experimental Section

All operations were performed under an inert atmosphere of a nitrogen-filled dry-box (Vacuum Atmospheres) or by using standard Schlenk techniques. All solvents were freshly distilled from the appropriate drying agent. Cy_2NH was distilled prior to use over molten potassium. NaH and *n*BuLi were used as received (Aldrich). Anhydrous $CrCl_3(THF)_3$ was prepared by reaction of $CrCl_3(H_2O)_6$ with TMS-Cl in THF.[13] Lithium biscyclohexylamide (Cy_2NLi) was prepared by treating a solution of Cy_2NH in hexane with a stoichiometric amount of *n*BuLi.[14a] (3,5-Me_2Ph)AdNLi (Ad = adamantyl),[14b] $[\{[(3,5\text{-}Me_2Ph)AdN]_2Cr\}_2]$[14c] and $[\{(Cy_2N)_2Cr\}_2]$[14d]

[*] S. Gambarotta, D. Reardon, I. Kovacs, K. B. P. Ruppa, K. Feghali
Department of Chemistry, University of Ottawa
Ottawa, Ontario K1N 6N5 (Canada)
Fax: Int. code +(613) 562-5170
sgambaro@orco.chem.uottawa.ca
J. Petersen
Department of Chemistry, West Virginia University
Morgantown, West Virginia, 26506-6045 (USA)

0947-6539/97/0309-1482 $ 17.50+.50/0

were prepared according to described procedures. IR spectra were recorded on a Michelson BOMEM FTIR instrument from Nujol mulls prepared in a dry-box. Elemental analyses were carried out with a Perkin Elmer 2000 CHN analyzer. The ratio between Cr and S atoms was determined by X-ray fluorescence on a Philips XRF 2400 instrument. Data for X-ray crystal structures were obtained with a Rigaku AFC6S diffractometer (Ottawa) and a Siemens P4 diffractometer (WVU). Mass spectra were obtained by a VG 7070 E spectrometer. Samples for magnetic susceptibility measurements were weighed inside a dry-box equipped with an analytical balance, and were sealed into calibrated tubes. Magnetic measurements were carried out with a Gouy balance (Johnson-Matthey) at room temperature. The magnetic moment was calculated following standard methods,[15] and corrections for underlying diamagnetism were applied to the data.[16] Variable-temperature magnetic measurements were performed at the Department of Chemistry of Memorial University (St. John's, Newfoundland) by using samples sealed in Teflon capsules under He atmosphere, and by using a Faraday balance.

Preparation of $[(Cy_2N)_3Cr]$ (1a): Freshly prepared Cy_2NLi (8.3 g, 44.1 mmol) was added to a slurry of $CrCl_3(THF)_3$ (5.1 g, 13.7 mmol) in toluene (150 mL) at −80 °C. The color slowly changed to dark brown upon mixing. The reaction mixture was stirred overnight at room temperature and filtered to eliminate a small amount of white solid. The volume of the resulting orange-brown mother liquor was reduced to a small volume. Slow cooling to −30 °C yielded dark brown crystals of **1a** (4.78 g, 8.1 mmol, 59%). Anal. calcd. (found) for $C_{36}H_{66}N_3Cr$: C 72.92 (73.39), H 11.22 (11.27), N 7.09 (6.92). IR [NaCl, Nujol mull, cm^{-1}]: $\tilde{\nu}$ = 1451 (s), 1341 (m), 1256 (m), 1189 (w), 1145 (m), 1112 (s), 1088 (s), 1039 (s), 961 (s), 917 (w), 887 (m), 841 (m), 801 (s), 780 (m), 699 (m), 638 (m), 621 (w), 582 (m). μ_{eff} = 3.81 μ_B. MS (EI): m/z = 592.2 $[(Cy_2N)_3Cr]^+$, 411.6 $[(Cy_2N)_2Cr]^+$, 329.3 $[(Cy_2N)(CyN)Cr]^+$, 232.7 $[(Cy_2N)Cr]^+$, 180.0 $[Cy_2N]^+$, 150.0 [(CyN)CrH].

Preparation of $[\{(3,5\text{-}Me_2Ph)AdN\}_3Cr]$ (1b): A solution of $CrCl_3(THF)_3$ (1.8 g, 4.8 mmol) in THF (125 mL) was treated with (3,5-Me_2Ph)AdNLi (5.1 g, 15.2 mmol) at ambient temperature. The color of the mixture rapidly changed to dark greenish brown. The reaction mixture was stirred for an additional 8 h and then evaporated to dryness. The residue was extracted with THF (100 mL) and then filtered to eliminate LiCl. The clean solution was concentrated and mixed with ether (100 mL). The resulting solution was cooled to −30 °C and allowed to stand for 2 d at low temperature, during which time crystals of **1b** separated (2.49 g, 2.94 mmol, 61%). Anal. calcd. (found) for $C_{54}H_{72}N_3Cr$: C 79.56 (79.22), H 8.90 (8.92), N 5.15 (4.57). IR [NaCl, Nujol mull, cm^{-1}]: $\tilde{\nu}$ = 1587 (s), 1351 (m), 1342 (w), 1298 (s), 1186 (w), 1160 (s), 1110 (s), 1089 (s), 1031 (m), 994 (s), 953 (s), 923 (s), 848 (m), 842 (m), 814 (w), 792 (w), 709 (m), 691 (s)). μ_{eff} = 3.97 μ_B. MS (FAB): m/z = 815.5 $[L_3Cr]^+$, 560.3 $[L_2Cr]^+$, 307.1 $[LCr]^+$.

Preparation of $[\{(Cy_2N)_2Cr\}_2(\mu\text{-}S)_2]$ (2a):

Method A: Crystalline sulfur (0.05 g, 1.7 mmol) was added to a dark brown solution of **1a** (1.0 g, 1.7 mmol) in toluene (100 mL) at room temperature. The mixture was stirred for 2 h and then filtered to remove any unreacted material. The resulting dark burgundy-red solution was allowed to stand at room temperature for 2 d yielding black crystals of **2a** (0.7 g, 0.78 mmol, 91%). Anal. calcd. (found) for $C_{48}H_{88}N_4S_2Cr_2$: C 64.82 (64.71), H 9.97 (9.73), N 6.30 (6.24). IR [NaCl, Nujol mull, cm^{-1}]: $\tilde{\nu}$ = 1359 (m), 1342 (m), 1259 (m), 1157 (w), 1138 (m), 1095 (s), 1030 (s), 978 (w), 954 (s), 891 (m), 844 (m), 801 (s), 699 (m). μ_{eff} = 2.15 μ_B per dimer. MS (FAB): m/z = 409.3 $[Cy_2N]_2^+$, 196.1 $[Cr_2S_2N_2]^+$, 168.1 $[Cr_2S_2]^+$.

Method B. A solution of $[\{(Cy_2N)_2Cr\}_2]$ (1.0 g, 1.2 mmol) in THF (100 mL) was treated with sulfur (80 mg, 2.5 mmol). The emerald green color of the solution changed instantly to red-brown, and after stirring overnight at room temperature, the solution was filtered and concentrated in vacuo. The resulting solution was allowed to stand at −30 °C for 1 d, during which time crystals of **2a** separated (0.9 g, 1.0 mmol, 84%). Analytical and spectroscopic data were in good agreement with those of the product obtained by method A.

Preparation of $[\{[(3,5\text{-}Me_2Ph)AdN]_2Cr(\mu\text{-}S)\}_2]$ (2b):

Method A [from **1b**]: A brownish-green solution of **1b** (1.4 g, 1.7 mmol) in THF (80 mL) was treated with sulfur (0.11 g, 0.4 mmol) at room temperature. The reaction mixture was refluxed for 2 d and then cooled to room temperature. After filtration, the solvent was removed in vacuo, and the solid residue was suspended in ether (30 mL). The solid rapidly dissolved and a brown crystalline **2b** separated upon allowing the solution to stand at room temperature for a few hours (0.3 g, 0.25 mmol, 30%). Anal. calcd. (found) for $C_{72}H_{96}N_4S_2Cr_2$: C 72.94 (72.78), H 8.16 (8.09), N 4.73 (4.61). IR [NaCl, Nujol mull, cm^{-1}]: $\tilde{\nu}$ = 1596 (s), 1356 (m), 1343 (w), 1303 (s), 1261 (s), 1186 (m), 1159 (s), 1081 (s), 1030 (s), 957 (w), 928 (w), 849 (w), 803 (s), 721 (w), 701 (s). μ_{eff} = 3.48 μ_B per dimer.

Method B (from $[\{(3,5\text{-}Me_2Ph)AdN]_2Cr\}_2]$. A solution of $[\{(3,5\text{-}Me_2Ph)AdN]_2Cr\}_2]$[14c] (1.5 g, 1.34 mmol) in THF (100 mL) was treated with sulfur (0.09 g, 0.3 mmol) at ambient temperature. In about 10 min the color of the solution changed from emerald green to brownish red. The solution was warmed to 55 °C and stirred for 5 h at that temperature. The reaction mixture was then cooled to room temperature, filtered and concentrated to a small volume of nearly 10 mL. Ether (about 50 mL) was added to the flask and the resultant solution was cooled to −30 °C. After 8 h standing at this temperature brown crystals of **2b** separated (0.8 g, 0.67 mmol, 50%). Spectroscopic and analytical data were in good agreement with those of the compound obtained from method A.

X-Ray Crystallography

Complex 1a: Data were collected at −153 °C. An air-sensitive crystal was mounted on a glass fiber inside a dry-box and transferred under the liquid nitrogen stream of the cooling system of a AFC6S Rigaku X-ray diffractometer. The ω–2θ scan technique was used to a maximum 2θ of 99.9°. Cell constants and orientation matrices were obtained from the least-squares refinement of 25 centered reflections. The intensities of three standard reflections, measured after every 150 reflections, showed no statistically significant decay over the duration of the data collections. Data were corrected for Lorentz and polarization effects and for absorption (DIFABS). The structure was solved by direct methods, which resulted in the location all the non-hydrogen atoms. Their positions were refined anisotropically. Hydrogen atom positions were calculated but not refined. Refinements were carried out by using full-matrix least-squares techniques on F, minimizing the function $\sum w(|F_o| - |F_c|)^2$, where $w = 1/\sigma^2(F_o^2)$ and F_o and F_c are the observed and calculated structure factors. Atomic scattering factors and anomalous dispersion terms were taken from the usual sources (Cromer & Waber).[17a] Anomalous dispersion effects were included in F_c. All calculations were performed using the TEXSAN (Molecular Structure Corporation) package on a Digital VAX station.

Complex 2a: A purple rectangular crystalline plate of **2a** was sealed under nitrogen in a capillary tube and then optically aligned on the goniostat of a Siemens P4 automated X-ray diffractometer. The corresponding lattice parameters and orientation matrix for the monoclinic unit cell were determined from a least-squares fit of the orientation angles of 30 reflections at 22 °C. Intensity data were measured with graphite-monochromated $Mo_{K\alpha}$ radiation (λ = 0.71073 Å) and variable ω scans (2.0–10.0° min^{-1}) for reflections within the detector range of $3.0 < 2\theta < 45°$. Background counts were measured at the beginning and at the end of each scan with the crystals and counter kept stationary. The intensities of three standard reflections were measured periodically during data collection to monitor crystal decomposition and instrument stability. The data were corrected for Lorentz-polarization effects and a face-indexed analytical absorption correction (T_{min} - T_{max} range: 0.895 to 0.957) was applied. The positions for the two independent Cr atoms and the remaining non-hydrogen atoms were initially determined by a combination of direct methods and difference Fourier calculations performed using the algorithms provided with the SHELXTL IRIS software running on a Silicon Graphics Iris Indigo workstation. Following anisotropic refinement of the non-hydrogen atoms, idealized positions for the hydrogen atoms were included at fixed contributions using a riding model. Full-matrix least-squares refinement, based upon the minimization of $\sum w_i|F_o - F_c|^2$, with $w_i^{-1} = \sigma^2(F_o) + 0.0008F_o^2$, converged to give final discrepancy indices[17b] of $R(F_o) = 0.0728$, $R_w(F_o) = 0.0754$ and $\sigma_1 = 1.43$ for 1484 reflections with $F_o > 4.0\sigma(F_o)$. The final difference map was essentially featureless.

Details on crystal data and structure solution for both **1a** and **2a** are given in Table 1. Selected bond lengths and angles are given in Table 2. Crystallographic data (including atomic coordinates and thermal parameters; excluding structure factors) for the structures reported in this paper have been deposited with the Cambridge Crystallographic Data Centre as supplementary publication no. CCDC-100350. Copies of the data can be obtained free of charge on application to The Director, CCDC, 12 Union Road, Cambridge CB2 1EZ, UK (Fax: Int. code +(1223)336-033; e-mail: deposit@chemcrys.cam.ac.uk).

  0947-6539/97/0309-1483 $ 17.50+.50/0

Table 1. Crystal data and structure analysis results for **1a** and **2a**.

	1a	**2a**
empirical formula	$C_{36}H_{66}CrN_3$	$C_{48}H_{88}Cr_2N_4S_2$
M_r	592.93	889.4
space group	$P2_1/n$	$P2/n$
a (Å)	10.712(1)	13.437(3)
b (Å)	19.486(2)	12.587(4)
c (Å)	17.185(2)	14.950(5)
β (°)	96.78(1)	95.96(2)
V (Å^3)	3562(1)	2514.8(13)
Z	4	4
λ (Å)	1.54178	0.71069
T (°C)	−153	295
ρ_{calcd} (g cm^{-3})	1.105	1.174
μ_{calcd} (cm^{-1})	28.47	5.49
R, R_w [a]	0.059, 0.058	0.073, 0.076

[a] $R = \sum||F_o| - |F_c||/\sum|F_o|$; $R_w = [(\sum(|F_o| - |F_c|)^2/\sum wF_o^2)]^{1/2}$.

Table 2. Selected bond lengths (Å) and angles (°).

Complex **1a**		Complex **2a**	
Cr1-N1	1.864(5)	Cr1-Cr2	2.821(4)
Cr1-N2	1.851(5)	Cr1-N1	1.803(10)
Cr1-N3	1.859(5)	Cr2-N2	1.806(10)
N1-C13	1.464(8)	Cr1-S1	2.174(4)
N1-C19	1.469(8)	Cr2-S1	2.179(4)
N1-Cr1-N2	119.9(2)	N1-C1	1.488(15)
N1-Cr1-N3	119.7(2)	N1-C7	1.493(14)
N2-Cr1-N3	120.4(2)	Cr2-Cr1-S1	49.7(1)
C13-N1-C19	113.3(5)	S1-Cr1-S1′	99.4(2)
Cr1-N1-C13	122.5(4)	Cr1-S1-Cr2	80.8(1)
Cr1-N1-C19	124.1(4)	N1-Cr1-N1′	112.0(6)
		N2-Cr2-N2′	112.4(6)
		C1-N1-C7	113.1(9)
		Cr1-N1-C1	131.4(7)
		Cr1-N1-C7	115.5(7)

Molecular Orbital Calculations: All molecular orbital calculations were performed on a Silicon Graphics computer by using the software package SPARTAN 4.0 (Wavefunction, Inc.; 18401 Von Karman Ave., #370, Irvine, CA 92715 USA, **1995**). The program's default parameters were used in the unrestricted Hartree-Fock ab initio calculations on the model compounds $[(Me_2N)_3Cr]$ and $[\{(Me_2N)_2Cr(\mu\text{-}S)\}_2]$ by using the STO-3G basis. The fractional atomic coordinates of the crystal structures were converted to the corresponding cartesian coordinates by using a special device of the NRCVAX program. The methyl group carbon atoms were deleted from the list and replaced with hydrogen atoms placed at their calculated positions. Minor adjustments were made to fit the geometry in the C_{3v} and C_{2v} symmetry classes.

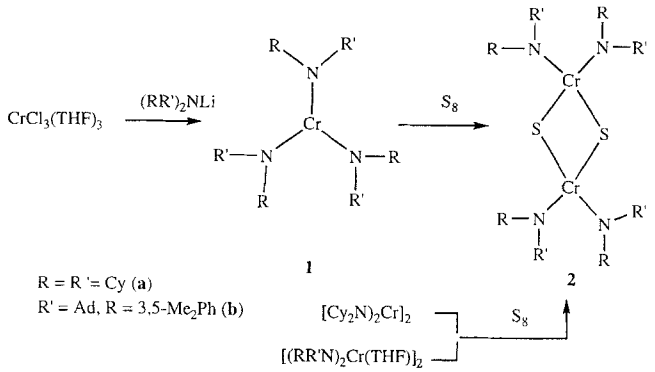

Scheme 1.

configuration of Cr^{III}, but still in the normal range. Complexes **1a,b** are highly soluble in hydrocarbons, and are extremely air and moisture sensitive. In agreement with the analytical data, the IR spectra did not show any absorption bands that might be attributed to coordinated THF. The mass spectra of both complexes showed the parent peaks in agreement with the proposed formulations, and fragmentation patterns consistent with the loss of RR′N units.

The molecular connectivity of **1a** was confirmed by an X-ray crystal structure. The complex is monomeric (Figure 1) with a

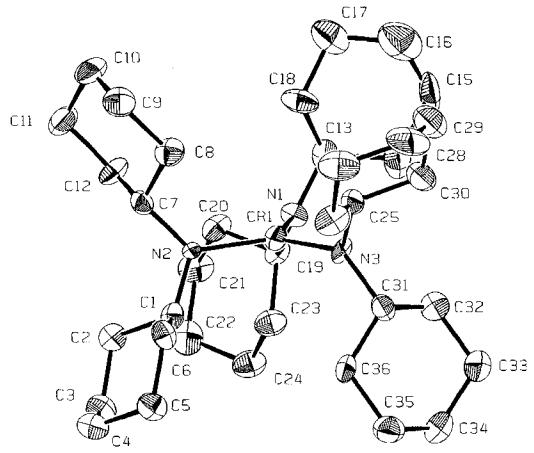

Figure 1. ORTEP plot of **1a**. Thermal ellipsoids are drawn at the 50% probability level.

Results and Discussion

The reaction of $CrCl_3(THF)_3$ with 3 equiv of $(RR')_2NLi$ [R = R′ = Cy; R = Ad, R′ = 3,5-Me_2Ph] in toluene (Scheme 1) resulted in a rapid color change from purple to dark brown. Dark brown, air-sensitive crystals of a paramagnetic complex formulated as $[(RR'N)_3Cr]$ [R = R′ = Cy (**1a**); R = Ad, R′ = 3,5-Me_2Ph (**1b**)] were obtained in reasonable yield after suitable workup and crystallization. The formulations were inferred from combustion analysis data. The magnetic moments were determined at room temperature and calculated on the basis of the proposed formulation (μ_{eff} = 3.81 and 3.97 μ_B for **1a** and **1b**, respectively). In the case of **1b** the value was found to be slightly higher than expected for the spin-only d^3 electronic

trigonal planar coordination geometry around the metal center defined by the three nitrogen atoms of the amide groups [N1-Cr1-N2 = 119.9(2)°, N1-Cr1-N3 = 119.7(2)°, N2-Cr1-N3 = 120.4(2)°]. The coordination geometry around each nitrogen atom is also trigonal planar [Cr1-N1-C13 = 122.5(4)°, Cr1-N1-C19 = 124.1(4)°, C13-N1-C19 = 113.3(5)°], consistent with sp^2 hybridization of the nitrogen atom. The short Cr–N distances [Cr1–N1 = 1.864(5) Å, Cr1–N2 = 1.851(5) Å, Cr1–N3 = 1.859(5) Å] also suggest the presence of a significant degree of Cr–N π-bond character. The three planes containing the three amide ligands are skewed with respect to each other and confer an overall propeller-shaped geometry around the chromium atom.[18a] From preliminary diffraction data it was also possible to obtain the molecular structure of complex **1b**.

0947-6539/97/0309-1484 $ 17.50+.50/0 Chem. Eur. J. 1997, 3, No. 9

Although the quality of the X-ray data for this analysis is marginal, it is sufficient to demonstrate the connectivity, the formula, and the presence of a very similar trigonal planar coordination geometry around the chromium atom.[18b]

The d^3 high-spin electronic configuration of the metal center was expected for complexes **1a,b**. In fact, either one of the C_3, C_{3v}, or D_{3h} symmetries, which may be reasonably assumed for the metal center, will maintain a sufficient level of degeneracy of the d orbitals to produce high-spin electronic configurations. An ab initio unrestricted Hartree–Fock molecular orbital calculation (UHF/STO-3G) was performed by the Spartan software package on the crystallographic geometry by replacing the large amide groups with Me_2N. The total energy of the molecule was calculated for both high-spin ($S = 3/2$) and low-spin ($S = 1/2$) configurations. The high-spin configuration was found to be the more stable by about 40 kcal mol^{-1}. Molecular orbitals were calculated for the 99 electrons of the molecule with a spin multiplicity of 4 (quartet state). The three unpaired electrons reside in three nearly degenerate orbitals.[19] As summarized in Scheme 2, the HOMO is primarily composed of contributions

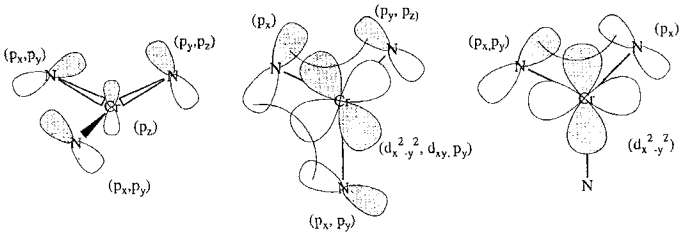

E (eV)	-0.206 (HOMO)	-0.248	-0.251

Scheme 2.

from the $4p_z$ atomic orbital of chromium with a slightly out-of-plane combination of the p_y and p_z orbitals of one nitrogen atom, and two in-plane combinations of both the p_x and p_y orbitals of each of the two other nitrogen atoms. This molecular orbital is essentially nonbonding with respect to the Cr–N bonds and is consistent with the charge distribution being localized primarily on the three nitrogen atoms. The second molecular orbital is mainly π in character with respect to the Cr–N bonds and arises from the interaction of an in-plane combination of p_y, $d_{x^2-y^2}$, and d_{xy} chromium atomic orbitals with three in-plane combinations of the p orbitals of the three nitrogen atoms. The third orbital corresponds to a π-bonding interaction between the chromium $d_{x^2-y^2}$ atomic orbital with two in-plane $p\pi$ orbitals of two nitrogen atoms. The complicated shape of these molecular orbitals can probably be ascribed to the particular propeller-like geometry adopted by the three ligands around the metal center. Calculations carried out on model compounds with same bond lengths and angles, but with a symmetry constrain to either C_{3v} or D_{3h}, showed that the three frontier orbitals are mainly formed by the three nitrogen p orbitals perpendicular to the molecular plane, with only a minor participation of the out-of-plane d orbitals of the metal center.

The EPR spectra in solution at room temperature show no resonance for **1a** and a broad and very weak resonance for **1b**. However, upon cooling a sharp and intense derivative signal ($g_\perp = 3.87$, **1a**; $g_\perp = 3.91$, **1b**) was observed for both complexes (Figure 2). Another weaker absorption band for **1a** was observed with an effective value of $g_\parallel = 1.99$. These features, consistent with the presence of an axial symmetry at chromium,

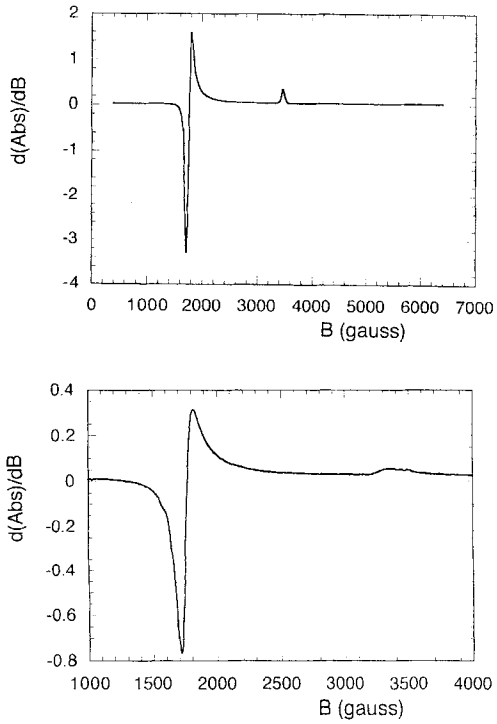

Figure 2. EPR spectra of **1a** and **1b** in frozen benzene solution at 100 K.

were also observed for solid state samples. The spectra did not show hyperfine structure arising from the coupling between the unpaired spin density on the Cr^{III} center and the amide nitrogens, which possess very little s character. This is likely to be the result of the trigonal planar coordination, which places the unpaired electrons in molecular orbitals that primarily involve π-bonding with the amide nitrogen p orbitals. As a result, the coupling between the unpaired electron spin on Cr and the ^{14}N nuclear spin through the Fermi contact mechanism is expected to produce a very small coupling for spin density delocalized on a p orbital of nitrogen. The EPR spectra are consistent with the results of the calculations described above; this shows that the three unpaired electrons are localized in three orbitals containing substantial in-plane nitrogen $p\pi$ contributions.

Reaction of **1a,b** with sulfur in toluene led to a minor color change from dark brown to dark reddish brown through a slow reaction (Scheme 1). Dark red crystals of two new compounds formulated as $[\{(RR'N)_2Cr\}_2(\mu\text{-}S)_2]$ (**2**) [R = R′ = Cy (**2a**); R = Ad, R′ = 3,5-Me_2Ph (**2b**)] were obtained by allowing the resulting solutions to stand at room temperature. The proposed formulations were consistent with combustion analysis and mass spectroscopy data. Although it was not possible to obtain a parent ion peak by using different ionization techniques, nevertheless, in both cases the spectra showed three intense peaks that can be attributed to $[(RR'N)_2Cr]^+$, $[N_2Cr_2S_2]^+$, and $[Cr_2S_2]^+$, respectively. These peaks also showed the expected isotopic distribution for chromium.

  0947-6539/97/0309-1485 $ 17.50+.50/0

Whereas our efforts to grow crystals of **2b** suitable for X-ray analysis were unsuccessful, the structure of **2a** was confirmed by an X-ray crystal structure. The molecular geometry of **2a** is constrained by a C_2 rotation axis, which passes through the two independent Cr atoms and bisects the two S-Cr-S angles (Figure 3). The two $(Cy_2N)_2Cr$ units are connected by two bridging

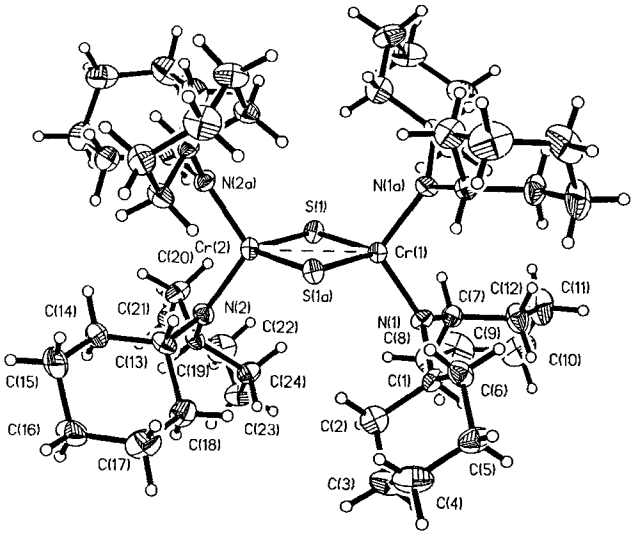

Figure 3. ORTEP plot of **2a**. Thermal ellipsoids are drawn at the 30% probability level.

sulfides forming a planar Cr_2S_2 core. The coordination geometry around the chromium atom is distorted tetrahedral and is defined by the two bridging sulfur atoms [Cr1–S1 = 2.174(4) Å, Cr2–S1 = 2.179(4) Å] and the nitrogen atoms of two terminal amide groups. The Cr–S distances are slightly shorter than those found in other sulfido- and persulfido-bridged mono-Cp Cr^{IV} compounds.[20] The short Cr–N distances [Cr1–N1 = 1.803(10) Å, Cr2–N2 = 1.806(10) Å] and the trigonal planar coordination geometry around each nitrogen atom [Cr1-N1-C1 = 131.4(7)°, Cr1-N1-C7 = 115.5(7)°, C1-N1-C7 = 113.1(9)°] reflects some degree of Cr–N π-bonding. The Cr_2S_2 core is perfectly planar with acute sharp angles subtended at the S atom [Cr1-S1-Cr2 = 80.8(1)°], which compare well with those of some sulfido-bridged organometallic systems.[20]

The reaction leading to the formation of **2a,b** involves the elimination of one amide ligand per chromium and is accompanied by an increase in the formal oxidation state of the Cr center from +3 to +4. So far our efforts to isolate and identify other species possibly present in the reaction mixture have been unsuccessful. It is reasonable to envision that the reaction mechanism proceeds with the formation of an intermediate pentavalent chromium complex $[(R_2N)_3Cr{=}S]$, from which the tetravalent complex **2** is obtained by reductive elimination of one amide radical.[9e] Consistent with this hypothesis, significant amount of free amine were detected by GC-MS in the mother liquor.

Complexes **2a,b** can also be produced in better yield by reaction of the corresponding Cr^{II} complexes with sulfur (Scheme 1). These reactions are rapid and do not require heating. To our surprise, complexes **2** are remarkably robust and are unreactive towards hydrogen, olefins, and CO.

The crystal structure of **2a** provides a rare example of non-Cp dinuclear Cr^{IV} compound.[20] The Cr–Cr distance [Cr1–Cr2 = 2.821(4) Å] together with the low magnetic moment [μ_{eff} = 2.15 μ_B *per dimeric unit* at room temperature] suggest the possible presence of an antiferromagnetic exchange or of a partial Cr–Cr bond. This in contrast to the case of the Cp^*Cr^{IV} sulfido derivatives which show significantly shorter intermetallic distances and for which the presence of Cr–Cr double bonds was proposed.[20] To investigate the nature of the Cr–Cr interaction in these species, magnetic susceptibility measurements over the temperature range of 4.5–300 K were carried out on samples of complexes **2a,b** by using a Faraday balance. From 75–300 K, the magnetic behavior deviates only slightly from the Curie–Weiss law (Figure 4). In this range of temperatures, the

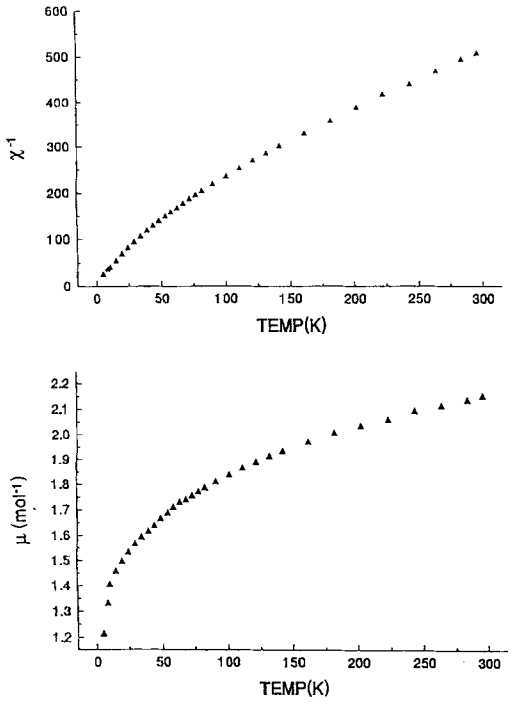

Figure 4. Diagram of the inverse of the molar magnetic susceptibility and of the magnetic moment as a function of the temperature for complex **2a**.

magnetic moment of **2a** varies from 2.15 to 1.80 μ_B. This behavior is somewhat reminiscent of that of monomeric and tetrahedral Cr^{IV} oxo derivatives which also show minor deviation from the Curie–Weiss law, and which are weakly antiferromagnetically coupled.[21] However, at about 50 K the magnetic moment decreases more rapidly to reach a value of 1.2 μ_B at 4.5 K. These data indicate that at temperatures above 50 K **2a** behaves as an almost regular paramagnet. The absence of an abrupt discontinuity in the variable-temperature magnetic susceptibility data, however, seems to rule out the possibility of antiferromagnetic coupling between the two paramagnetic Cr^{IV} centers of **2a**. The observed decline in μ_{eff} from 1.8 to 1.2 μ_B may more likely reflect a change in the relative populations of the triplet and singlet spin populations associated with each d^2 Cr^{IV} center. By comparison, the magnetic moment of **2b** at room temperature of 3.48 μ_B

0947-6539/97/0309-1486 $ 17.50+.50/0 *Chem. Eur. J.* **1997**, *3*, No. 9

is significantly larger than that of **2a**. Similarly, the magnetic susceptibility of **2b** obeys the Curie–Weiss law ($\theta = -49$ K) within the temperature range 60–200 K (Figure 5). As the temperature is lowered, the magnetic susceptibility decreases gradually toward zero, thus showing a behavior reminiscent of antiferromagnetism. However, the complexity of the observed magnetic behavior suggests that several different phenomena may be contributing to producing the temperature dependence of the magnetic moments of **2a** and **2b**.

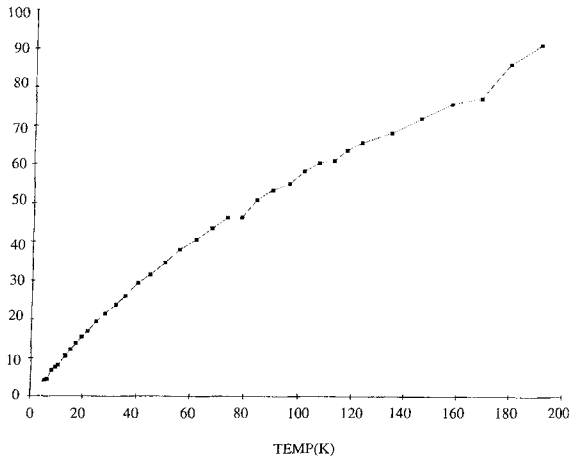

Figure 5. Diagram of the inverse of the molar magnetic susceptibility as a function of the temperature for complex **2b**.

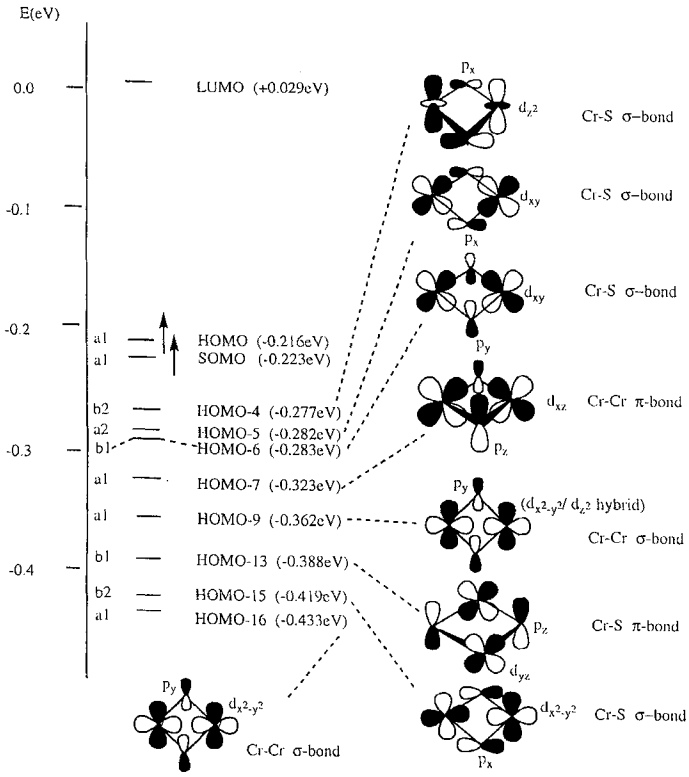

Figure 6. Energy-level diagram for $[\{[(CH_3)_2N]_2Cr\}_2(\mu\text{-}S)_2]$ showing the most relevant Cr–S and Cr–Cr molecular orbitals.

In an effort to clarify the magnetic behavior and the nature of the Cr–Cr interaction in **2a,b**, ab initio UHF/STO-3G calculations were performed on the model complex $[\{(Me_2N)_2Cr(\mu\text{-}S)\}_2]$, with the atomic coordinates of the non-hydrogen atoms obtained from the X-ray crystal structure of **2a**. Given the value of the magnetic moment, the triplet state was considered to be the most reasonable basis for the calculations (calculations carried out on the quintet state yielded a significantly higher value of the total energy). The result showed a rather small HOMO–LUMO gap of 0.245 eV, which may well account for the low paramagnetism. The two unpaired electrons are located in two frontier orbitals, namely, the HOMO (−0.216 eV) and the next lower MO [HOMO −1 (−0.223 eV)]. The near degeneracy of these two orbitals nicely explains the significant decrease of the magnetic moment observed at low temperatures. These two orbitals are centered on Cr–N with a weak Cr–S antibonding character. The bonding of the Cr_2S_2 core is mainly realized with five molecular orbitals. Four of them [HOMO −4 (−0.277 eV), HOMO −5 (−0.282 eV), HOMO −6 (−0.283 eV), HOMO −15 (−0.419 eV)] possess a marked σ character with respect to the Cr–S bond, while the fifth one [HOMO −13 (−0.388 eV)] is mainly a Cr–S π bond. As illustrated in Figure 6, the four Cr–S σ bonds are originated by the chromium d orbitals (or hybrid combinations) with in-plane p orbitals of the bridging sulfide. Conversely, the Cr–S π bond is formed by the two out-of-plane d_{yz} chromium orbitals with p_z of the two bridging sulfur. Three more MO's also are Cr–S bonds, but display some significant Cr–Cr bond character. Two of them [HOMO −9 (−0.362 eV) and HOMO −16 (−0.433 eV)] are reminiscent of Cr–Cr σ bonds. The two orbitals are similar in shape and are formed by the overlap of the sulfur p_y orbitals with either the $d_{x^2-y^2}$ or a hybrid combination of d_{z^2} with $d_{x^2-y^2}$ orbitals of the two chromium atoms. Both orbitals are characterized by the presence of a large lobe delocalized between the four core atoms and may be regarded as Cr–Cr σ bonds. However, the participation of the bridging atoms atomic orbitals is very substantial. A third orbital (HOMO −7) located at −0.323 eV is formed by the overlap of the sulfur p_z with the two d_{zx} orbitals of the two chromium atoms; two large lobes on the two sides of the Cr_2S_2 core result. This MO may be regarded as a sort of Cr–Cr π bond which, again, involves the atomic orbitals of the bridging sulfur atoms in a rather important manner.

These observations indicate that the electronic coupling between the two d^2 Cr atoms may involve mechanisms other than direct M–M bond or antiferromagnetic exchange. While the direct Cr–Cr interaction appears to be weak and certainly unable to hold together the dinuclear frame in the absence of bridging atoms, the Cr–Cr "bonds" made with the determinant participation of the bridging atom orbitals provide a rather efficient coupling between the two metal centers and, ultimately, are probably responsible for the low magnetic moments. Clearly, all the bonding interactions in the molecule concur to determine the HOMO–LUMO gap and consequently the magnetic properties of the complex. The sharp lowering of the magnetic moment observed at low temperatures is probably due to changes in the relative spin populations resulting from the near degeneracy of the two highest occupied molecular orbitals. In addition, since the participation of the atomic orbitals of the bridging atoms (and also of the amide nitrogen atoms) is crucial

  0947-6539/97/0309-1487 $ 17.50+.50/0

to the formation of three MO's with Cr–Cr character, even small modification of the geometry of the ligand system will change their relative stability as well as the size of the HOMO–LUMO gap. This may well explain the difference in magnetic moments observed for the two isostructural compounds **2a,b**. Obviously theoretical calculation are needed in each individual case in order to make these assessments.

Acknowledgments: This work was supported by the National Science and Engineering Council of Canada (NSERC) through a strategic and operating grant. We are grateful to Dr. L. Thompson (Memorial University, Newfoundland) for the variable-temperature magnetic measurements on complex **2a**, Dr. D. Wilcox (Dartmouth College) for the assistance in the interpretation of the EPR spectra, and Dr. J. Lamarche (Ottawa) for recording the EPR spectra. J. L. P. acknowledges the financial support provided by the Chemical Instrumentation Program of the National Science Foundation (Grant no. CHE-9120098) for the acquisition of a Siemens P4 X-ray Diffractometer by the Department of Chemistry at West Virginia University.

Received: February 26, 1997 [F625]

[1] a) L. F. Larkworthy, K. B. Nolan, P. O'Brien in *Comprehensive Coordination Chemistry*, 2nd ed. (Eds.: E. W. Abel, F. G. A. Stone, G. Wilkinson), Pergamon, **1985**. b) M. J. Winter, S. Woodward in *Comprehensive Organometallic Chemistry*, 2nd ed. (Eds.: E. W. Abel, F. G. A. Stone, G. Wilkinson), Pergamon **1995**, Vol. 5. c) S. W. Kirtley in *Comprehensive Organometallic Chemistry* (Eds.: E. W. Abel, F. G. A. Stone, G. Wilkinson), Pergamon **1982**, Vol. 3. d) D. C. Bradley, M. H. Chisholm, *Acc. Chem. Res.* **1976**, *9*, 273. e) K. H. Theopold, *ibid.* **1990**, *23*, 263.

[2] See for example: a) J. W. Buchler, K. L. Lay, L. Castle, V. Ullrich, *Inorg. Chem.* **1982**, *21*, 842. b) D. A. House, C. F. Garner, *Nature (London)* **1965**, *208*, 776. c) L. C. Yuan, T. C. Bruice, *J. Am. Chem. Soc.* **1985**, *107*, 512. d) J. T. Groves, J. W. Kruper Jr, R. C. Haushalter, W. M. Butler, *Inorg. Chem.* **1982**, *21*, 1363. e) P. Stavropoulos, P. D. Savage, R. P. Tooze, G. Wilkinson, B. Hussain, M. Motevalli, M. B. Hursthouse, *J. Chem. Soc. Dalton Trans.* **1987**, 557. f) S. E. Creager, R. W. Murray, *Inorg. Chem.* **1985**, *24*, 3824. g) D. J. Liston, B. O. West, *ibid.* **1985**, *24*, 1568. h) C. J. Cardin, D. J. Cardin, A. Roy, *J. Chem. Soc. Chem. Commun.* **1978**, 899. i) A. R. Barron, J. E. Salt, G. Wilkinson, M. Motevalli, M. B. Hursthouse, *J. Chem. Soc. Dalton Trans.* **1987**, 2947. j) J. E. Salt, G. S. Girolami, G. Wilkinson, M. Motevalli, M. Thornton-Pett, M. B. Hursthouse, *ibid.* **1985**, 685.

[3] See for example: a) K. Srinivasan, J. J. Kochi, *Inorg. Chem.* **1985**, *24*, 4671. b) M. Krumpolc, J. Rocek, *J. Am. Chem. Soc.* **1979**, *101*, 3206. c) M. Mitewa, P. R. Bontchev, *Coord. Chem. Rev.* **1985**, *61*, 241. d) N. Nag, R. N. Bose, *Struct. Bonding (Berlin)* **1985**, *63*, 153. e) S. K. Noh, R. A. Heintz, B. S. Haggerty, A. L. Rheingold, K. H. Theopold, *J. Am. Chem. Soc.* **1992**, *114*, 1892. f) R. A. Heintz, R. L. Ostrander, A. L. Rheingold, K. H. Theopold, *ibid.* **1994**, *116*, 11387. g) D. B. Morse, T. B. Rauchfuss, S. R. Wilson, *ibid.* **1988**, *110*, 8234. h) H. Lam, G. Wilkinson, B. Hussain-Bates, M. B. Hursthouse, *J. Chem. Soc. Dalton Trans.* **1993**, 1477.

[4] a) F. A. Cotton, G. Wilkinson, *Advanced Inorganic Chemistry*, 5th ed., Wiley, New York **1988**. b) J. K. Beattie, G. P. Haight, *Progr. Inorg. Chem.* **1972**, *20*, 93. c) G. P. Haight, J. H. Tracy, B. Z. Shakashiri, *J. Inorg. Nucl. Chem.* **1971**, *33*, 2169.

[5] See for example: a) S. L. Scott, A. Bakac, J. H. Espenson, *J. Am. Chem. Soc.* **1992**, *114*, 4205. b) S. L. Scott, A. Bakac, J. H. Espenson, *Inorg. Chem.* **1991**, *30*, 4112.

[6] See for example: a) J. Muzart, *Chem. Rev.* **1992**, *92*, 113. b) G. Cainelli, G. Cardillo, *Chromium Oxidations in Organic Chemistry*; Springer, Berlin **1984**. c) L. E. Martinez, J. L. Leighton, D. H. Carsten, E. N. Jacobsen, *J. Am. Chem. Soc.* **1995**, *117*, 5897.

[7] See for example: a) K. W. Jennette, *Biol. Trace Elements Res.* **1979**, *1*, 55. b) B. Gulanowski, J. Swiatek, H. Kozlowski, *J. Inorg. Biochem.* **1992**, *48*, 289. c) A. Kortenkamp, G. Oetken, D. Beyersmann, *Mutation Res.* **1990**, *232*, 155.

[8] See for example: a) K. J. Liu, X. Shi, J. J. Jiang, F. Goda, N. Dalal, H. M. Swartz, *Arch. Biochem. Biophys.* **1995**, *323*, 33. b) P. H. Connett, K. E. Wetterhanh, *Struct. Bonding* **1983**, *54*, 93. c) K. W. Jennette, *J. Am. Chem. Soc.* **1982**, *104*, 874. d) S. C. Rossi, N. Gorman, K. E. Wetterhanh, *Chem. Res. Toxicol.* **1988**, *1*, 101. e) X. Shi, N. S. Dalal, *Arch. Biochem. Biophys.* **1990**, *277*, 342. f) X. Shi, Z. Dong, N. S.Dalal, P. M. Gannett, *Biochim. Biophys. Acta* **1994**, *226*, 65. g) X. Lin, Z. Zhuang, M. Costa, *Carcinogenesis* **1992**, *13*, 1763. h) M. Cieslak-Galonka, *Polyhedron* **1996**, *15*, 3667.

[9] a) R. L. LaDuca, P. T. Wolczanski, *Inorg. Chem.* **1992**, *31*, 1311. b) C. E. Laplaza, A. L. Odom, W. M. Davis, C. C. Cummins, J. D. Protasiewicz, *J. Am. Chem. Soc.* **1995**, *117*, 4999. c) C. C. Cummins, R. R. Schrock, W. M. Davis, *Organometallics* **1992**, *11*, 1452. d) P. Berno, S. Gambarotta, *Angew. Chem. Int. Ed. Engl.* **1995**, *34*, 822. e) L. Scoles, K. B. Ruppa, S. Gambarotta, *J. Am. Chem. Soc.* **1996**, *118*, 2529. f) L. Scoles, R. Minhas, R. Duchateau, J. Jubb, S. Gambarotta, S. *Organometallics* **1994**, *13*, 4978. g) P. Berno, S. Hao, R. Minhas, S. Gambarotta, *J. Am. Chem. Soc.* **1994**, *116*, 7417. h) J. I. Song, P. Berno S. Gambarotta *J. Am. Chem. Soc.* **1994**, *116*, 6927. i) P. Berno, S. Gambarotta, *Organometallics* **1994**, *13*, 2569. j) P. Berno, R. Minhas, S. Hao, S. Gambarotta *ibid.* **1994**, *13*, 1052.

[10] C. E. Laplaza, C. C. Cummins, *Science* **1995**, *268*, 861.

[11] a) A. L. Odom, C. C. Cummins, *J. Am. Chem. Soc.* **1995**, *117*, 6613. b) G. K. Barker, M. F. Lappert, J. A. K. Howard, *Chem. Soc. Dalton Trans* **1977**, 734. c) J. C. W. Chien, W. Kruse, D. C. Bradley, C. W. Newing, *J. Chem. Soc. Chem. Commun.* **1970**, 1177.

[12] M. Dionne, J. Jubb, H. Jenkins, S. Wong, S. Gambarotta, *Inorg. Chem.* **1996**, *35*, 1874.

[13] P. Boudjouk, J. H. So, *Inorg. Synth.* **1992**, *29*, 108.

[14] a) J. Jubb, P. Berno, S. Hao, S. Gambarotta, *Inorg. Chem.* **1995**, *34*, 3563. b) K. B. Ruppa, S. Gambarotta, A. L. Rheingold, G. Yap, *Inorg. Chem.* **1997**, *36*, 1194. c) K. B. P. Ruppa, S. Gambarotta, unpublished results. d) J. J. H. Edema, S. Gambarotta, A. Meetsma, A. L. Spek, W. W. J. Smeets, M. Y. Chiang, *J. Chem. Soc. Dalton Trans.* **1993**, 789.

[15] M. B. Mabbs, D. J. Machin, *Magnetism and Transition Metal Complexes* Chapman and Hall; London, **1973**.

[16] G. Foese, C. J. Gorter, L. J. Smits, *Constantes Selectionnées Diamagnetisme, Paramagnetisme, Relaxation Paramagnetique*. Masson, Paris **1957**.

[17] a) D. T. Cromer, J. T. Waber, *International Tables for X-ray Crystallography*, The Kynoch Press, Birmingham, England 1974. b) The discrepancy indices were calculated from the expressions $R(F_o) = \sum|F_o - F_c|/\sum F_o$ and $R_w(F_o) = \sum(w_i)^{1/2}|F_o - F_c|/\sum(w_i)^{1/2}F_o$, and the standard deviation of an observation of unit weight σ_1 is equal to $[(\sum w_i|F_o - F_c|^2)/(n-p)]^{1/2}$, where n is the number of observations and p is the number of parameters varied during the last refinement cycle.

[18] a) The geometry appears to be rather similar to that of the recently reported tris-silazanate chromium complex. R. D. Köln, G. K. Köln, M. Haufe. *Chem Ber.* **1996**, *129*, 25. b) Crystal data for **1b** are as follows: $C_{54}H_{72}N_3Cr$. F. W. 815.18, monoclinic $P2_1/c$, $a = 18.767(2)$, $b = 12.515(3)$, $c = 20.761(4)$ Å, $\beta = 108.72(2)^\circ$, $V = 4622.9(1)$ Å^3, $Z = 4$, $\rho_{calcd} = 1.067$ g cm^{-3}, $F_{000} = 1477$, $\mu = 27.00$ cm^{-1}, $T = -153\,^\circ$C, $R = 0.095$, $R_w = 0.106$, GOF = 0.85 for 522 parameters and 8241 reflections out of 11890 unique.

[19] The axis perpendicular to the molecular plane was chosen as the z axis. The Cr–N vectors were chosen as x axis for the local nitrogen coordinates.

[20] For a few example of dinuclear Cr^{IV} cyclopentadienly derivatives see: a) H. Brunner, J. Pfauntsch, J. Wachter, B. Nuber, M. L. Ziegler, *J. Organomet. Chem.* **1989**, *559*, 179. b) L. Y. Goh, T. C. W. Mak, *J. Chem. Soc. Chem. Commun.* **1986**, 1474. c) H. Brunner, J. Wachter, E. Guggolz, M. L. Ziegler, *J. Am. Chem. Soc.* **1982**, *104*, 1765.

[21] B. L. Chamberlain, M. P. Herrero-Fernandez, T. A. Hewston, *J. Solid State Chem.* **1985**, *59*, 111.

  0947-6539/97/0309-1488 $ 17.50+.50/0